Spontaneous and UVR-induced multiple metastatic melanomas in *Cdk4*$^{R24C/R24C}$/*TPras* mice

Elke Hacker*, H. Konrad Muller+, Nicole Irwin*, Brian Gabrielli#, Douglas Lincoln*, Sandra Pavey*, Marianne Broome Powell#, Marcos Malumbres^, Mariano Barbacid^, Nicholas Hayward*, Graeme Walker*

*Queensland Institute of Medical Research, Brisbane, Queensland, Australia

^Molecular Oncology, Centro Nacional de Investigaciones Oncológicas, Madrid, Spain

+University of Tasmania, School of Medicine, Hobart, Tasmania, Australia

#Division of Radiation and Cancer Biology, Stanford University, Stanford, California

#Centre for Immunology and Cancer Research, Brisbane, Queensland, Australia

Running title: UVR-induced melanomas in *Cdk4*$^{R24C/R24C}$/*TPras* mice

Keywords: transgenic mouse, metastatic melanoma, ultraviolet radiation, Ras, Cdk4

Corresponding author: Graeme Walker, PhD

Queensland Institute of Medical Research

300 Herston Rd, Herston

QLD 4006, Australia

E-mail: graemeW@qimr.edu.au

Ph: 61-7-33620308

Fax: 61-7-38453508

Abstract

Human melanoma susceptibility is often characterized by germline inactivating *CDKN2A* (INK4A/ARF) mutations, or mutations that activate CDK4 by preventing its binding to and inhibition by INK4A. We have previously shown that a single neonatal UVR dose delivered to mice that carry melanocyte-specific activation of Hras (*TPras*) increases melanoma penetrance from 0 to 57%. Here we report that activated *Cdk4* cooperates with activated *Hras* to greatly increase susceptibility to melanoma in mice. While UVR treatment failed to induce melanomas in $Cdk4^{R24C/R24C}$ mice, it greatly increased the penetrance and decreased the age of onset of melanoma development in $Cdk4^{R24C/R24C}$/*TPras* animals, compared to *TPras* alone. This increased penetrance was dependant on the threshold of Cdk4 activation, as $Cdk4^{R24C/+}$/*TPras* animals did not show an increase in UVR-induced melanoma penetrance compared to *TPras* alone. In addition, $Cdk4^{R24C/R24C}$/*TPras* mice invariably developed multiple ~~primary~~ lesions, which occurred rarely in *TPras* mice. These results indicate that germline defects abrogating the pRb pathway may enhance UVR-induced melanoma. *TPras* and $Cdk4^{R24C/R24C}$/*TPras* tumors were comparable histopathologically, but the latter were larger and more aggressive, and cultured cells derived from such melanomas were also larger and had higher levels of nuclear atypia. Moreover, the melanomas in $Cdk4^{R24C/R24C}$/*TPras* mice, but not *TPras* mice, readily metastasized to regional lymph nodes. Thus it appears that in the mouse, *Hras* activation initiates UVR-induced melanoma development, while the cell cycle defect introduced by mutant *Cdk4* contributes to tumor progression, producing ~~larger,~~ more aggressive, metastatic tumors.

Introduction

In some transgenic strains of mice [*Mt-Hgf/Sf* (1); and *TPras* (2, 3)], a single erythemal UVR dose of 9kJ/m^2 to 2-4 day old neonates, induces melanoma development with greatly increased penetrance compared to chronic UVR treatments to adult mice of the same genotype. In humans, melanoma susceptibility is often characterised by mutations of *CDKN2A* (which encodes $p16^{INK4A}$ and $p14^{ARF}$) and *CDK4*. INK4A is a CDK-inhibitor that binds to and inhibits CDK4 (and CDK6), which otherwise phosphorylates pRb and induces G1-S phase progression. ARF acts through a distinct pathway involving stabilization of p53 through abrogation of MDM2-induced p53 degradation (4). Underlining the importance of *CDK4* in melanoma susceptibility are germline *CDK4* mutations (R24C or R24H) in some melanoma kindreds (5, 6) that render it resistant to INK4A inhibition. It is unclear if such mutations are functionally equivalent to deletion of INK4A, as other inhibitors ($p15^{INK4B}$, $p18^{INK4C}$ and $p19^{INK4D}$) are also capable of binding and inhibiting CDK4, and their interaction is also thought to be abrogated by the R24C mutation.

Ras/Raf/MAPK pathway activation is also critical for melanoma development. The MAPK pathway is activated through mutation of *BRAF* in 62-72% of sporadic melanomas and by *RAS* mutations in about 10% (7, 8). The relationship between MAPK activation and UVR exposure is complex. *BRAF* mutations are rarely found in mucosal and acral melanomas (i.e. those not associated with sun-exposure) (9, 10). Interestingly, neither are they found commonly in areas of chronic UVR exposure (e.g. the face, where *NRAS* mutations are more likely), but are often found in melanomas from areas of intermittent sun exposure (e.g. the back and trunk) (10). Despite differences in specificity between Ras family members, mice carrying mutations either in *Hras* (2, 3) or *Nras* (11) develop melanoma. Further *in vivo* evidence for the role of *Braf* in melanocyte neoplasia comes from zebrafish, where *Braf* mutations induce nevus formation and cooperate with p53-deficiency to induce melanoma (12).

Mice carrying specific ablation of either *Ink4a* (13, 14) or *Arf* (15) rarely develop melanoma spontaneously (reviewed (16)). However melanocyte-specific activation of *Hras* on both *Ink4* and *Arf*-null backgrounds leads to spontaneous melanoma development (17), but with only locally invasive, non-metastatic tumors. As an additional model for human melanoma, *Cdk4* has also been targeted in mice, by homologous recombination to "knock in" the activating R24C mutation (18). These animals are prone to cancer as they age but do not develop melanomas unless exposed to potent carcinogens (19). Interesting inroads have been made into the relative roles of the pRb and p53 pathways in UVR-induced melanoma development in mice (17). UVR treatment increases melanoma penetrance in *Arf*$^{-/-}$*/Tyr-Hras* but not *Ink4a*$^{-/-}$*/Tyr-Hras* animals. Thus, in mice at least, germline mutations resulting in pRb pathway dysregulation may eliminate the melanoma-inducing effects of UVR. Spontaneous melanomas in *Arf*$^{-/-}$*/Tyr-Hras* animals have a high degree of chromosomal instability, while UVR-induced lesions are cytogenetically intact except for frequent genomic amplification targeting *Cdk6* (17). To further assess the role of the pRb pathway in murine melanoma development we have assessed spontaneous and UVR-induced melanoma in *Cdk4-R24C* mutant mice that also carry melanocyte-specific activated *Hras*.

Materials and Methods

All experiments were undertaken with the approval of the QIMR Animal ethics committee (approval number A98004M).

Mouse strains.

Cdk4$^{R24C/R24C}$ mice have been previously described (18). *Tyr-Hras (G12V*) transgenic mice (*TPras*) express mutant (G12V) Hras in a melanocyte-specific manner via a tyrosinase gene promoter/enhancer cassette (2). All mice were on a mixed SV129/C3H background.

UVR treatments.

At day 2-4, animals were irradiated with a single UVR dose of 8.15 kJ/m^2 as described previously (3).

Cell Culture and Morphology.

Tumors were digested in 1.2 U/ml Dispase (Invitrogen, Carlsbad, CA), and cultured in RPMI (GIBCO, Carlsbad, CA), supplemented with 10% fetal bovine serum (CSL Limited, Australia). Cell lines were grown on cover-slips, and DNA and microtubules were examined by fluorescence microscopy as previously described (20).

FACS Analysis

Cells were fixed in 70% ethanol and stained with propidium iodide (Molecular Probes, Carlsbad, CA). The ploidy status was determined using the FACCalibur (BD bioscience, Franklin Lakes, NJ) cell sorter and data analyzed with Modfit Software (Verity, Topsham, ME). Ploidy status was determined by comparing the profile of diploid lymphocytes to that of the melanoma cell lines.

Immunohistochemistry (IHC).

Paraffin-embedded sections of melanomas were dewaxed, and antigen retrieval performed using citrate buffer, pH 6.0. Endogenous peroxidase activity was quenched in 3% H_20_2 for 10 min, and sections were then washed and blocked with 10% goat serum. The primary antibodies were a p16 polyclonal antibody (SC-1207, Santa Cruz Biotechnology, Santa Cruz, CA) applied at 1:300 dilution, a p53 polyclonal antibody (CM5, Novocastra, UK) applied at 1:500, a tyrosinase-related protein 1 (Tyrp1, αPEP1) polyclonal antibody diluted 1:500 (a gift from Dr V.J. Hearing), a rabbit anti-caspase 3 (Biocare Medical, Concord, CA) diluted 1:500 and a biotin-labeled anti-MCM7 mouse monoclonal diluted 1:250 (Neomarkers, Freemont, CA). Secondary detection was via an Envision plus detection kit (DAKO, Denmark), which was visualized using AEC plus (DAKO), and sections were counterstained with haematoxylin.

PCR, RT-PCR and Sequencing Analysis.

DNA and RNA were extracted using Qiagen kits (Qiagen, Germany). *Cdkn2a* copy number was assessed by multiplex PCR with exon-specific primers using *Gapdh* as a control (supplementary Fig 1). Levels of *Ink4a*, *Arf*, *Cdk6* and *c-Myc* expression were determined by SYBR Green (Qiagen) real-time quantitative PCR. cDNA was made using Superscript II reverse transcriptase (Invitrogen), and subsequent PCR reactions were carried out on a Rotorgene 3000 cycler (Corbett Research, Australia). Data was analyzed using Rotorgene 6 software as previously described (21). *β-Actin* was used as a PCR control, and expression in melanomas and cell lines was compared to that in wild-type skin. Sequencing was performed using BigDye Terminator 3 methodology (ABI Prism, Foster City, CA) on a 3100 Genetic Analyzer (ABI Prism). Data was analyzed using SeqDoC software (22). Primers were designed to amplify the entire 1709 bp *Trp53* cDNA (open reading frame) in 3 overlapping fragments, and were located in sequences that are not

shared with the *Trp53* pseudogene on chromosome 17. All primer sequences available (supplementary data Table I).

Statistical Analysis

The survival of mice in each treatment group was estimated using Kaplan-Meier analysis, and the log-rank test was used to test for pairwise differences between the groups. The associations between treatment and the proportion of mice that developed disease characteristics were tested using pairwise Fisher's exact tests or Mann-Whitney U tests. The statistical significance levels for all tests were adjusted for the multiple pairwise comparisons using the Bonferroni method.

Results

$Cdk4^{R24C/R24C}$/*TPras* mice develop multiple spontaneous and UVR-induced melanomas.

We compared penetrance of melanoma at one year in $Cdk4^{R24C/R24C}$, $Cdk4^{R24C/R24C}$/*TPras*, $Cdk4^{R24C/+}$/*TPras* mice, after a single neonatal UVR dose of 8.15 kJ/m^2, with untreated mice of the same genotype as controls. Fig. 1D shows the Kaplan-Meier curve for tumor-free mice at one year of age. $Cdk4^{R24C/R24C}$ mice did not develop melanoma spontaneously or after neonatal UVR. As reported previously (3), *TPras* mice developed neonatal UVR-induced, but not spontaneous melanomas (Fig. 1D). However, 58% of mice homozygous for the *Cdk4*-R24C mutation, and also carrying the melanocyte-specific activated *Hras* ($Cdk4^{R24C/R24C}$/*TPras*), developed melanoma spontaneously. UVR treatments increased the penetrance of tumor development to 83% (and from 0-40% for $Cdk4^{R24C/+}$/*TPras* mice), and decreased the estimated age of onset compared to untreated animals (Fig. 1D) Lesions were mainly dermal melanomas. They were often multicentric, had aberrant nuclear features, and were usually accompanied by epidermal hyperplasia in UVR-treated animals (Fig. 2A). The increased melanoma susceptibility in mice carrying both activated *Cdk4* and *Hras* is underlined by their increased propensity to develop multiple primary melanomas. All melanoma-bearing UVR-treated $Cdk4^{R24C/R24C}$/*TPras* animals developed more than one primary lesion, significantly more than untreated $Cdk4^{R24C/R24C}$/*TPras* mice (40%, p= 0.012, Fisher exact test, Bonferroni adjustment) or UVR-treated *TPras* mice (16%, p= 0.001)(Fig. 1A).

Mice carrying activated *Cdk4* and *Hras* develop aggressive metastatic melanomas.

Cohorts carrying both mutant *Cdk4* and *Hras* were also more likely than *TPras* animals to develop lymph node metastases (Fig. 1B). Metastases, defined as enlarged draining lymph nodes that stained for Tyrp1, were seen in 92% (12/13) of tumor-bearing UVR-

treated *Cdk4*$^{R24C/R24C}$*/TPras*; 60% (3/5) of spontaneous *Cdk4*$^{R24C/R24C}$*/TPras*, and 16% (1/6) of UVR-treated *TPras* animals respectively. All metastases involved only the draining lymph node, with no evidence of visceral dissemination. Small numbers of scattered Tyrp1-positive cells were sometimes observed in the lymph nodes of melanoma-free *TPras* mice. However mice with enlarged nodes generally had a single macrometastasis; these ranged in size from approximately 400-1000 cells. The *Cdk4*$^{R24C/R24C}$*/TPras* (+UVR) cohort had a higher rate of metastatic melanoma than the *TPras* (+UVR) cohort (p= 0.001, Fisher exact test, Bonferroni adjustment). In addition to being more prone to development of metastases, the primary lesions on the UVR-treated *Cdk4*$^{R24C/R24C}$*/TPras* were on average larger than those carried by the *TPras* animals (Fig. 1C), although the difference fell just short of significance (p= 0.057).

We hypothesized that tumors in the mice carrying the *Cdk4* defect may be more aggressive because of a cell cycle control defect introduced by pRb pathway deregulation, hence we examined cultured melanoma cells from various genotypes for evidence of mitotic defects (Fig. 3A). Nuclei in cultured *TPras* melanoma cells ranged from 7-18 μm in diameter, whereas nuclei from *Cdk4*$^{R24C/R24C}$*/TPras* tumors were 20-70 μm in diameter. Additionally, the latter cultures had a higher proportion of multinuclear cells, and generally larger cytoplasmic and nuclear volume than the *TPras* cells. We also assessed DNA content in two cell lines where low melanin content permitted FACS analysis (Fig. 3B). The *TPras* cell line was diploid, while the *Cdk4*$^{R24C/R24C}$*/TPras* cell line was aneuploid. To confirm that this difference in nuclear size was not simply an artefact of culture, we also measured nuclear size in tumor sections. The nuclei in tumors from *TPras* animals were smaller than those in *Cdk4*$^{R24C/R24C}$*/TPras* melanomas (Mann-Whitney U test $p<0.01$) (Fig. 3C, D). Interestingly, nuclei in the *TPras* primary tumor cells (range 2.5-15 μm) were within the same size range as those in corresponding cultured *TPras* melanoma cells (7-18 μm), whereas nuclei in cultured *Cdk4*$^{R24C/R24C}$*/TPras* melanoma cells (20-70 μm) were

considerably larger than their *in vivo* tumor counterparts (4-20 μm). The additional increase in nuclear size of *Cdk4*$^{R24C/R24C}$*/TPras* melanoma cells in culture presumably reflects their transition to aneuploidy, which did not occur in *TPras* cultures.

To further assess phenotypic parameters that may explain the differences in aggressiveness between *Cdk4*$^{R24C/R24C}$*/TPras* and *TPras* tumors, we scored proliferation, apoptosis and vascularity in melanoma sections (Fig. 2B). Tumors from UVR-treated *Cdk4*$^{R24C/R24C}$*/TPras* mice had significantly greater blood vessel density than that of *TPras* (+UVR) tumors (Mann-Whitney U test, $p<0.01$), in keeping with the fact that *TPras* melanomas are small *in situ* lesions (Fig. 4A). Moreover, there were more proliferating cells in the UVR-induced *Cdk4*$^{R24C/R24C}$*/TPras* melanomas than in the UVR-induced *TPras* tumors although this fell just short of significance (Mann-Whitney U test, $p = 0.078$) (Fig. 4B). There was no significant difference in the level of apoptosis between any of the cohorts (Fig. 4C).

Molecular changes in *Cdk4*$^{R24C/R24C}$*/TPras* melanomas.

Genomic PCR and real-time qRT-PCR were used to assess the relative copy number of *Ink4a* and *Arf* genes respectively. In addition to testing the melanomas, we also analyzed cell lines generated from them, to confirm that stromal contamination did not mask loss of *Ink4a* or *Arf*. No loss of either gene or their transcripts was seen in tumors (N=17) or cell lines (N=12) from mice of any cohort carrying the *Cdk4-R24C* mutation. We also stained tumor sections for Ink4a by IHC (supplementary Fig 2). Ink4a immunoreactivity was observed in 31/35 (89%) samples (Table I).

We also stained for Trp53 protein in tumors and found that 36/56 (64%) of the melanomas were positive (Table I). However, we rarely observed Trp53 staining in spontaneous *Cdk4*$^{R24C/R24C}$*/TPras* melanomas (2/8), whereas it was present in the majority of UVR-induced *Cdk4*$^{R24C/R24C}$*/TPras* tumors (25/35). Trp53 reactivity was generally

sparse, moderately intense, nuclear staining, such as observed in the UVR-treated skin used as a positive control (Fig. 2C). Thus this Trp53 staining in our tumors probably represents upregulation of the protein in some tumor cells in response to cellular deregulation or damage. In some Trp53-positive tumors, staining was more intense and occasionally cytoplasmic. This staining seemed to be specific to the UVR-induced tumors, as it was observed in 11/35 (31%) *Cdk4*$^{R24C/R24C}$*/TPras* (+UVR) compared to 0/8 spontaneous *Cdk4*$^{R24C/R24C}$*/TPras* melanomas. We hypothesized that such high expression may have been indicative of a mutant Trp53, as has been shown in other studies of mouse melanomas (23). However, sequencing of the entire *Trp53* open reading frame in 7/11 of these high Trp53 expressing tumors revealed no mutations, thus the mode of p53 dysregulation in these lesions is unknown. It should be noted that the lack of staining for Ink4a or Trp53 does not necessarily mean loss of expression, as neither protein can be detected by IHC in unchallenged wild-type mouse skin.

We also examined expression of *c-Myc* and *Cdk6,* which have been previously shown to be upregulated by gene amplification (>2-fold relative to melanocytes) in some mouse melanomas (17, 24). This was assessed by qRT-PCR, with results expressed relative to wild-type skin (normalized to a value of 1). *c-Myc* expression was significantly higher (p= 0.041, Mann-Whitney U test) in spontaneous *Cdk4*$^{R24C/R24C}$*/TPras* lesions (mean= 1.9, N= 3) than UVR-induced melanomas of the same genotype (mean=0.892, N= 8) (Table I). Neither cohort showed significant amplification of *Cdk6* over wild-type levels (UVR-induced *Cdk4*$^{R24C/R24C}$*/TPras*; mean= 0.786, N= 8, and spontaneous *Cdk4*$^{R24C/R24C}$*/TPras*; mean= 1.13, N= 3).

Discussion

It has been previously found (17) that following UVR, mice carrying a pRb pathway defect, together with melanocyte-specific activation of *Hras* (*Ink4a*$^{-/-}$*/Tyr-Hras*), do not show an increase in melanoma development over spontaneous levels, indicating that pRb pathway defects may not be required for UVR-induced melanoma. Our data for *Cdk4*$^{R24/+}$*/TPras* heterozygous mice adds some support for this conclusion since *Cdk4*$^{R24/+}$*/TPras* animals developed UVR-induced melanoma with the same penetrance as mice carrying only activated Hras (*TPras*). This indicates that their melanoma development is being driven by activated Ras alone. However, when in a homozygous state, the *Cdk4* mutation did increase melanoma penetrance in mice following UVR. *Cdk4*$^{R24/R24C}$*/TPras* mice developed melanomas with significantly greater incidence and earlier onset than the *TPras* animals (Fig. 1D), suggesting that involvement of the pRb pathway in UVR-induced melanoma may depend on a particular threshold of pRb pathway deregulation. Involvement of pRb pathway abrogation in UVR-induced melanoma development is not unexpected as some studies have indicated a role for pRb in DNA repair. *In vitro* studies with *Ink4a* and *Arf*-null murine embryonic fibroblasts (25) have shown that, at least in that cell type, pRb pathway abrogation results in a significant diminution of DNA repair capacity (interestingly there was little difference between *Ink4*$^{-/-}$ and *Arf*$^{-/-}$ cells).

The penetrance of UVR-induced melanoma in *TPras* transgenics on an *Arf* or *trp53*-null background is unknown. However *Arf*$^{-/-}$*/Tyr-Hras* mice (17) developed UVR-induced melanomas with greater penetrance than our similarly treated *Cdk4*$^{R24C/R24C}$*/TPras* mice (80% compared to 40% at 150 days). We predict that *Arf*$^{-/-}$*/TPras* (or *Trp53*$^{-/-}$*/TPras*) mice may have an even earlier age of onset than *Arf*$^{-/-}$*/Tyr-Hras* because of the higher expression of Hras in our *TPras* transgenics, compared to the *Tyr-Hras* transgenics of others (17). This would suggest that *Arf*$^{-/-}$*/TPras* (or *Trp53*$^{-/-}$*/TPras*) mice would develop melanomas with a greater penetrance and earlier onset than our *Cdk4*$^{R24/R24C}$*/TPras*

animals, and thus a p53 pathway defect would still be more effective at inducing melanoma in this model.

Another possible explanation for the difference between our study and that of Kannan et al, (17) is that the use of activated *Cdk4* (at least in the homozygous state) ultimately has a different functional effect than Ink4a ablation. In *Ink4a* knockout mice other members of the same family of cyclin-dependent kinase inhibitors (i.e. Ink4b, Ink4c, Ink4d) may be able to compensate to some degree for Ink4a loss. In contrast, homozygosity for the activated Cdk4 would over-ride such inhibitor redundancy. Evidence for such redundancy comes from studies with mice null for another Ink4 inhibitor, Ink4c (19). These animals develop significantly more carcinogen-induced melanocytic lesions than controls, indicating that, in addition to Ink4a, Ink4c also plays a role in suppressing melanocyte transformation via regulation of Cdk4. This argument for inhibitory redundancy is supported by our results showing that the wild type copy of *Cdk4* carried by our *Cdk4*$^{R24/+}$*/TPras* cohort seems to play a role in protecting against initiation of UVR-induced melanoma. We found no evidence of loss of the wild type allele in the *Cdk4*$^{R24/+}$*/TPas* melanomas (data not shown). This is to be expected if, as we suggest, the tumor development is primarily being driven by the activated Ras.

Further highlighting the cooperativity between activated Cdk4 and UVR, the UVR-treated animals more often presented with multiple primaries, and generally developed larger lesions than those in *TPras* animals although there were no obvious histopathological differences between spontaneous and UVR-induced melanomas from *Cdk4*$^{R24/R24C}$*/TPras* mice. The differences in aggressiveness seem to be due to a higher degree of cell proliferation in tumors carrying the mutant Cdk4, as there was no significant difference in tumor cell apoptosis between genotypes. In addition, the *Cdk4*$^{R24C/R24C}$*/TPras* melanomas had a significantly greater density of blood vessels than *TPras* lesions. although we suspect that this is primarily due to the fact that the tumors carrying mutant

Cdk4 are on average much larger than the *in situ* lesions which predominate in the *TPras* mice. In keeping with their aggressive phenotype, UVR-induced *Cdk4*$^{R24C/R24C}$*/TPras* tumors had larger nuclei than those from *TPras* animals and their corresponding cell lines exhibited other evidence of mitotic defects including aneuploidy, increased nuclear size heterogeneity and the appearance of multinuclear cells.

Concomitant abrogation of the pRb and p53 pathways is a hallmark of mouse melanomas (17, 23). We saw no evidence of loss of *Ink4a* in the *Cdk4*$^{R24C/R24C}$*/TPras* tumors, as may be expected because the pRb pathway is already deregulated by the constitutively active *Cdk4*. Gain of chromosome 15, with resultant over-expression of *c-Myc*, has previously been observed in spontaneous *Trp53*$^{-/-}$*/Tyr-Hras* melanomas (24). This was not observed in *Ink4a*$^{-/-}$*/Tyr-Hras* tumors (17), indicating that it may be an alternative method of abrogating the pRb axis, given that *c-Myc* over-expression alone can cause loss of the G1 cell cycle transition via activation of either Cdk2 or Cdk4 complexes (26). We observed *c-Myc* upregulation in some spontaneous melanomas, consistent with the results of Bardeesy *et al.* (24), indicating that high levels of *c-Myc* expression is sometimes observed in melanomas regardless of whether they are induced on a background of pRb or p53 pathway deficiency. Notably, this was not observed in UVR-treated melanomas in our study, nor by Kannan *et al.* (17), indicating that c-Myc deregulation may be limited to spontaneous melanoma.

Cdk6 amplification is another avenue of pRb pathway deregulation in mouse melanoma, and is a marker for UVR-induced melanoma in *Arf*$^{-/-}$*/Tyr-Hras* mice, with *Cdk6*-amplified tumors showing greater than 2-fold increase in expression compared to mouse melanocytes (17). None of our melanomas attained this level of overexpression. Thus *Cdk6* upregulation does not appear to be a marker of UVR-induced melanoma in our strains, and its amplification may be specific to UVR-induced melanomas generated on *Arf* or *Trp53*-null backgrounds.

We also looked for evidence of p53 pathway inactivation but found no loss of *Arf* at the genomic or transcriptional level in any melanomas generated on the *Cdk4-R24C* background. This might be expected, as *Arf* is usually co-deleted with *Ink4a* at the *Cdkn2a* locus, and in our models there is no selective pressure for such loss as the pRb pathway is already inactivated by mutant *Cdk4*. However we often observed Trp53 expression in tumors that was never observed in non-treated wild-type skin and is probably due to cellular stress or p53 pathway deregulation. Trp53 expression was observed more often in UVR-induced than in spontaneous tumors (Table I). High over-expression, not associated with Trp53 mutation, but possibly indicative of further p53 dysregulation or resistance to degradation, was invariably found only in UVR-induced tumors. This is consistent with other studies (17) indicating that in mice carrying a pRb pathway defect, deregulation of the p53 pathway may be involved in melanoma development, further underlining the significant role for p53 pathway deregulation in UVR-induced melanoma.

In summary, we have shown that inactivation of the pRb pathway by mutant Cdk4 in mice also carrying melanocyte-specific Hras activation, leads to the development of multiple metastatic melanomas. The exposure of these mice to a single neonatal UVR treatment significantly increases the penetrance and decreases the age of onset of tumors, indicating that in this model, abrogation of the pRb pathway affects response to UVR. Our results are suggestive of a model where pRb pathway defects increase susceptibility to UVR-induced melanoma.

Acknowledgements

This work was funded by the Queensland Cancer Fund.

References

1. Noonan FP, Recio JA, Takayama H, Duray P, Anver MR, Rush WL, et al. Neonatal sunburn and melanoma in mice. Nature 2001;413(6853):271-2.

2. Broome Powell M, Gause PR, Hyman P, Gregus J, Lluria-Prevatt M, Nagle R, et al. Induction of melanoma in TPras transgenic mice. Carcinogenesis 1999;20(9):1747-53.

3. Hacker EI, N. Muller, HK. Broome Powell, M. Kay, GF. Hayward, NK. Walker, GJ. Neonatal ultraviolet radiation exposure is critical for malignant melanoma induction in pigmented TPras transgenic mice. J. Invest. Dermatol 2005;125(5):1074-1077.

4. Zhang Y, Xiong Y, Yarbrough WG. ARF promotes MDM2 degradation and stabilizes p53: ARF-INK4a locus deletion impairs both the Rb and p53 tumor suppression pathways. Cell 1998;92(6):725-34.

5. Molven A, Grimstvedt MB, Steine SJ, Harland M, Avril MF, Hayward NK, et al. A large Norwegian family with inherited malignant melanoma, multiple atypical nevi, and CDK4 mutation. Genes Chromosomes Cancer 2005;44(1):10-8.

6. Zuo L, Weger J, Yang Q, Goldstein AM, Tucker MA, Walker GJ, et al. Germline mutations in the p16INK4a binding domain of CDK4 in familial melanoma. Nat Genet 1996;12(1):97-9.

7. de Snoo FA, Hayward NK. Cutaneous melanoma susceptibility and progression genes. Cancer Lett 2005;230(2):153-86.

8. Dong J, Phelps RG, Qiao R, Yao S, Benard O, Ronai Z, et al. BRAF oncogenic mutations correlate with progression rather than initiation of human melanoma. Cancer Res 2003;63(14):3883-5.

9. Cohen Y, Rosenbaum E, Begum S, Goldenberg D, Esche C, Lavie O, et al. Exon 15 BRAF mutations are uncommon in melanomas arising in nonsun-exposed sites. Clin Cancer Res 2004;10(10):3444-7.

10. Maldonado JL, Fridlyand J, Patel H, Jain AN, Busam K, Kageshita T, et al. Determinants of BRAF mutations in primary melanomas. J Natl Cancer Inst 2003;95(24):1878-90.

11. Ackermann J, Frutschi M, Kaloulis K, McKee T, Trumpp A, Beermann F. Metastasizing melanoma formation caused by expression of activated N-RasQ61K on an INK4a-deficient background. Cancer Res 2005;65(10):4005-11.

12. Patton EE, Widlund HR, Kutok JL, Kopani KR, Amatruda JF, Murphey RD, et al. BRAF mutations are sufficient to promote nevi formation and cooperate with p53 in the genesis of melanoma. Curr Biol 2005;15(3):249-54.

13. Krimpenfort P, Quon KC, Mooi WJ, Loonstra A, Berns A. Loss of p16Ink4a confers susceptibility to metastatic melanoma in mice. Nature 2001;413(6851):83-6.

14. Sharpless NE, Bardeesy N, Lee KH, Carrasco D, Castrillon DH, Aguirre AJ, et al. Loss of p16Ink4a with retention of p19Arf predisposes mice to tumorigenesis. Nature 2001;413(6851):86-91.

15. Kamijo T, Zindy F, Roussel MF, Quelle DE, Downing JR, Ashmun RA, et al. Tumor suppression at the mouse INK4a locus mediated by the alternative reading frame product p19ARF. Cell 1997;91(5):649-59.

16. Walker GJ, Hayward NK. Pathways to melanoma development: lessons from the mouse. J Invest Dermatol 2002;119(4):783-92.

17. Kannan K, Sharpless NE, Xu J, O'Hagan RC, Bosenberg M, Chin L. Components of the Rb pathway are critical targets of UV mutagenesis in a murine melanoma model. Proc Natl Acad Sci U S A 2003;100(3):1221-5.

18. Rane SG, Dubus P, Mettus RV, Galbreath EJ, Boden G, Reddy EP, et al. Loss of Cdk4 expression causes insulin-deficient diabetes and Cdk4 activation results in beta-islet cell hyperplasia. Nat Genet 1999;22(1):44-52.

19. Sotillo R, Garcia JF, Ortega S, Martin J, Dubus P, Barbacid M, et al. Invasive melanoma in Cdk4-targeted mice. Proc Natl Acad Sci U S A 2001;98(23):13312-7.

20. Gabrielli BG, De Souza CP, Tonks ID, Clark JM, Hayward NK, Ellem KA. Cytoplasmic accumulation of cdc25B phosphatase in mitosis triggers centrosomal microtubule nucleation in HeLa cells. J Cell Sci 1996;109 (Pt 5):1081-93.

21. Pfaffl MW. A new mathematical model for relative quantification in real-time RT-PCR. Nucleic Acids Res 2001;29(9):e45.

22. Crowe ML. SeqDoC: rapid SNP and mutation detection by direct comparison of DNA sequence chromatograms. BMC Bioinformatics 2005;6(1):133.

23. Sharpless NE, Kannan K, Xu J, Bosenberg MW, Chin L. Both products of the mouse Ink4a/Arf locus suppress melanoma formation in vivo. Oncogene 2003;22(32):5055-9.

24. Bardeesy N, Bastian BC, Hezel A, Pinkel D, DePinho RA, Chin L. Dual inactivation of RB and p53 pathways in RAS-induced melanomas. Mol Cell Biol 2001;21(6):2144-53.

25. Sarkar-Agrawal P, Vergilis I, Sharpless NE, DePinho RA, Runger TM. Impaired processing of DNA photoproducts and ultraviolet hypermutability with loss of p16INK4a or p19ARF. J Natl Cancer Inst 2004;96(23):1790-3.

26. Dang CV. c-Myc target genes involved in cell growth, apoptosis, and metabolism. Mol Cell Biol 1999;19(1):1-11.

Figure legends

Figure 1. Melanoma penetrance and phenotypic characteristics. A, Bar graph displaying the percent of melanoma-bearing animals that developed multiple primary melanomas. B, Percent of melanoma-bearing animals that developed melanoma metastases. C, Proportion of melanoma-bearing animals that developed lesions of over 1 cm^2 in size. D, Kaplan-Meier curve estimating the time to spontaneous and UVR-induced melanoma development in the various genetically modified mice. Animals that died without developing melanoma are represented by a black dash. There was a significant difference in melanoma penetrance between the UVR-treated *Cdk4*$^{R24C/R24C}$*/TPras* (Cdk4$^{R/R}$/TPras) cohort, and the UVR-treated *Cdk4*$^{R24C/+}$*/TPras* (Cdk4$^{R/+}$/TPras), *TPras*, and spontaneous *Cdk4*$^{R24C/R24C}$*/TPras* cohorts ($p<0.001$, log rank test). The age of mice was defined by the appearance of cutaneous melanoma and additional signs of morbidity.

Figure 2. Histological staining of melanoma sections. A, H&E stained section of a cutaneous melanoma exhibiting hyperplasia of the epidermis (left image), that was frequency observed in UVR-treated animals. Pigmented tumor cells were frequently observed in lymph nodes (centre image), and the right image shows Tyrp1-positive tumor cells staining red (scale bar= 0.1mm). B, Sections of melanomas stained for MCM7 (left), Caspase 3 (middle) and H&E (right) (scale bar= 0.1 mm), the latter image shows several clearly visible blood vessels containing red blood cells. C, Immunohistochemical staining of Trp53 in non-treated wild-type mouse skin (left) (scale bar= 0.1 mm), UVR-treated wild-type mouse skin (middle) (scale bar= 0.1 mm) and melanoma lesion (right) (scale bar= 50 μm).

Figure 3. Nuclei atypia in melanoma cells carrying mutant Cdk4. A, Representative images of tumor cell lines stained for DNA (Hoechst) and microtubules (α-tubulin). The nucleus size ranged from 7-18 μm in *TPras* (+UVR) cells (2 images on left) and between 20-70 μm in *Cdk4/$^{R24C/R24C}$/TPras* (+UVR) cells (two images on right) (scale bar= 50 μm). B, The two histograms on the left show the *TPras* (+UVR) melanoma cell line (the first is cell line alone and the second is cell line spiked with lymphocytes). The two histograms on the right show the *Cdk4/$^{R24C/R24C}$/TPras* (+UVR) melanoma cell line (the second is spiked with lymphocytes). The *TPras* (+UVR) cell line is diploid and the *Cdk4/$^{R24C/R24C}$/TPras* (+UVR) cell line is aneuploid. C, Average size of nuclei in melanomas from *Cdk4/$^{R24C/R24C}$/TPras* (+UV) and *TPras* (+UV) mice. Nuclear size was determined by measuring H&E stained sections. 50 cells over 5 fields from each melanoma were counted from the two genotypes (number of tumors counted shown in graph). D, Average percent of nuclei per tumor greater than 10 μm for both genotypes.

Figure 4 Tumor aggressiveness in *Cdk4$^{R24C/R24C}$/TPras* and *TPras* melanomas.

Mean and standard error of the mean of (A) blood vessels per field (X200) in ten randomly selected fields per tumor; (B) proliferating cells (MCM7 staining) per field (X400) in ten randomly selected fields per tumor; (C) apoptotic cells (cleaved caspase 3 staining) per field (X400) in ten randomly selected fields per tumor. Mean and standard error are shown.

	qRT-PCR		Immunohistochemistry			Sequence
Strain	Cdk6 upreg	c-Myc upreg	Ink4a	Trp53	Trp53 upreg	Trp53 mutations
TPras/Cdk4$^{R/R}$ +UV						
Melanomas	0% n=8	0% n=8	86% n=29	71% n=35	31% n=35	0% n=7
Melanoma cell lines	ND	ND	ND	ND		0% n=1
TPras/Cdk4$^{R/R}$ -UV						
Melanomas	0% n=3	66% n=3	78% n=9	25% n=8	0% n=8	0% n=3
Melanoma Cell line	ND	ND	ND	ND		ND
TPras/Cdk4$^{R/+}$ +UV						
Melanomas	0% n=1	0% n=1	100% n=5	83% n=6	67% n=6	ND
Melanoma Cell line	ND	ND	ND	ND		ND
TPras +UV						
Melanomas	ND	0% n=3	71% n=7	57% n=7	29% n=7	ND
Melanoma Cell line	ND	ND	ND	ND		ND

Table I **Molecular analysis of melanomas.** Quantitative real-time PCR (qRT-PCR) was used to detect c-Myc and Cdk6 over-expression in melanoma samples. Samples were assessed to be over-expressing (upreg) these genes if the expression level was 2-fold that of wild-type skin.

ND = not done

Figure 1

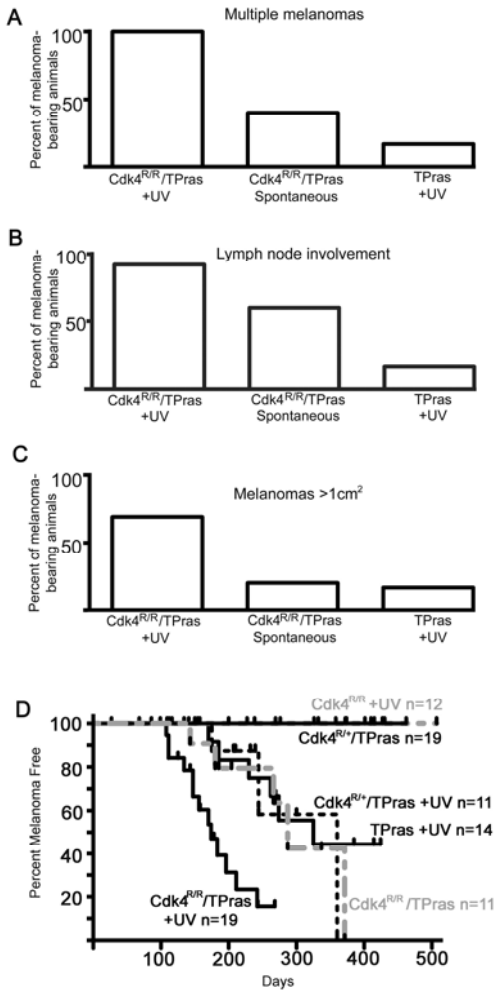
A
Multiple melanomas
Percent of melanoma-bearing animals
100
50
Cdk4R/R/TPras +UV
Cdk4R/R/TPras Spontaneous
TPras +UV
B
Lymph node involvement
Percent of melanoma-bearing animals
100
50
Cdk4R/R/TPras +UV
Cdk4R/R/TPras Spontaneous
TPras +UV
C
Melanomas >1cm2
Percent of melanoma-bearing animals
100
50
Cdk4R/R/TPras +UV
Cdk4R/R/TPras Spontaneous
TPras +UV
D
Cdk4R/R +UV n=12
Cdk4R/+/TPras n=19
Cdk4R/+/TPras +UV n=11
TPras +UV n=14
Cdk4R/R /TPras n=11
Cdk4R/R/TPras +UV n=19
Percent Melanoma Free
100
80
60
40
20
100
200
300
400
500
Days

Figure 2

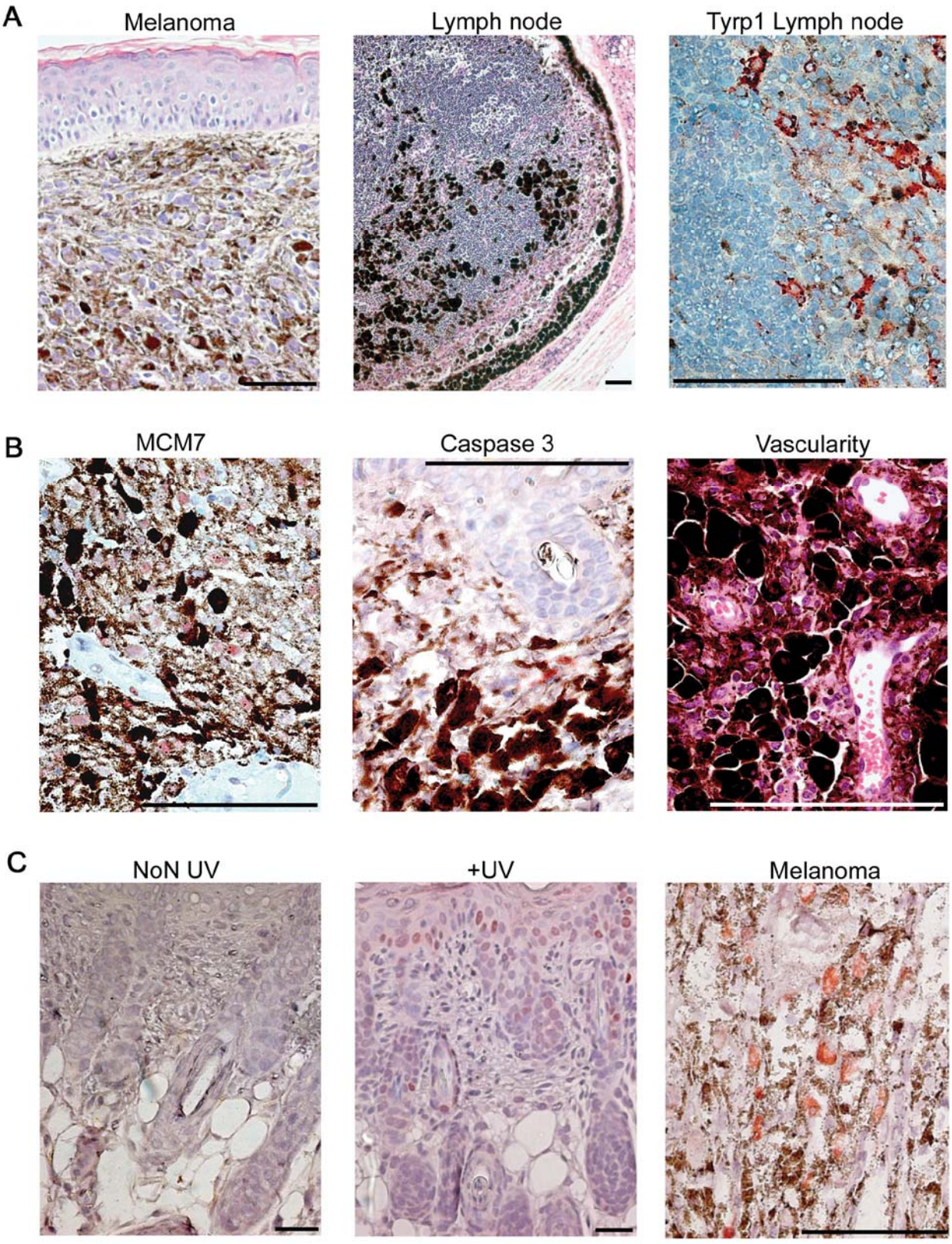
A
Melanoma
Lymph node
Tyrp1 Lymph node
B
MCM7
Caspase 3
Vascularity
C
NoN UV
+UV
Melanoma

Figure 3

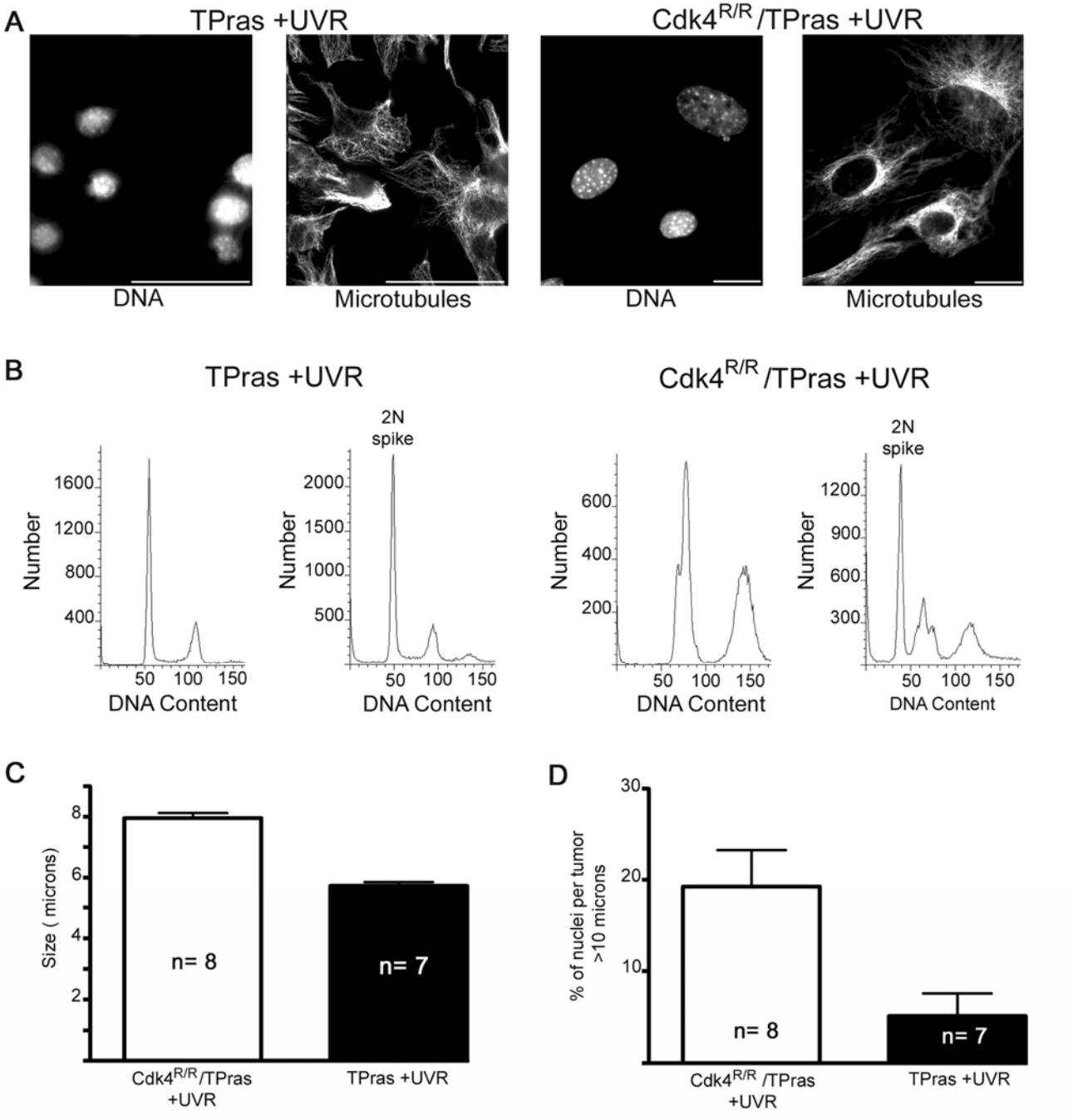
A
TPras +UVR
Cdk4R/R /TPras +UVR
DNA
Microtubules
DNA
Microtubules
B
TPras +UVR
Cdk4R/R /TPras +UVR
2N spike
Number
DNA Content
2N spike
Number
DNA Content
Number
DNA Content
2N spike
Number
DNA Content
C
Size (microns)
n= 8
n= 7
Cdk4R/R/TPras +UVR
TPras +UVR
D
% of nuclei per tumor >10 microns
n= 8
n= 7
Cdk4R/R /TPras +UVR
TPras +UVR

Figure 4

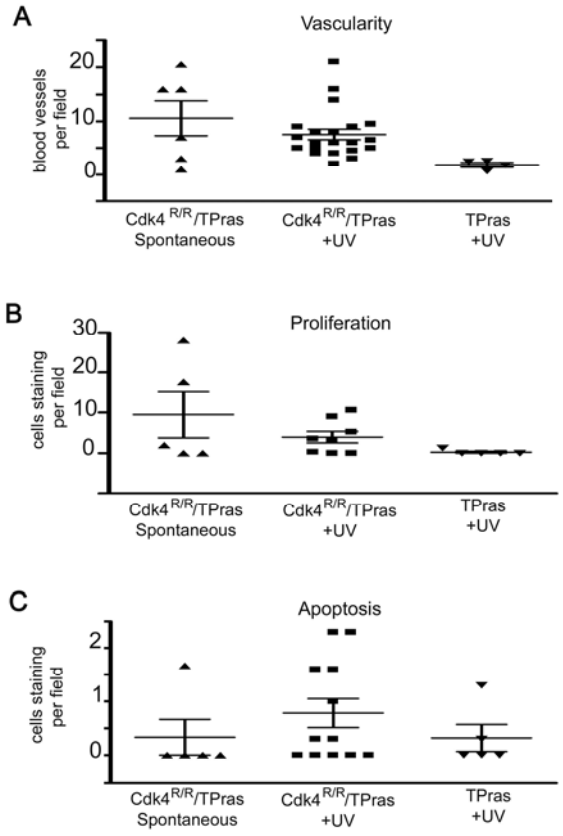
A
Vascularity
blood vessels per field
20
10
0
Cdk4 R/R/TPras Spontaneous
Cdk4R/R/TPras +UV
TPras +UV
B
Proliferation
cells staining per field
30
20
10
0
Cdk4R/R/TPras Spontaneous
Cdk4R/R/TPras +UV
TPras +UV
C
Apoptosis
cells staining per field
2
1
0
Cdk4R/R/TPras Spontaneous
Cdk4R/R/TPras +UV
TPras +UV